MODELING ANTENNA COUPLING AND CORRELATION IN RAPIDLY FADING MIMO CHANNELS

Jon W. Wallace[1] **and Michael A. Jensen**[2]

[1]*School of Engineering and Science, International University of Bremen, D-28759 Bremen, Germany*
[2]*Department of Electrical and Computer Engineering, Brigham Young University, Provo, UT 84602, USA*

ABSTRACT

Node mobility in rich multipath environments limits the quality of attainable channel state information (CSI) due to wavelength-scale fading, leading to effectively lower channel capacities. Recent work on the capacity of block-fading MIMO channels considers the impact of antenna correlation at the transmitter [1], proving that correlation guarantees capacity growth with additional antennas and suggests that for rapidly fading channels, antennas should be paced as close together as possible. This work augments the MIMO modeling strategy in [1] to include the effects of electromagnetic coupling of the antennas. Constraining the radiated power of the transmit array reveals that the reported gains result from simple beamforming mechanisms, and that capacity growth only comes from increased *channel* correlation, not *antenna* correlation whose gain is offset by increased coupling. The new model also predicts that optimal antenna placement for rapidly fading channels is not arbitrarily close, but rather on the order of 0.3 to 0.6 wavelengths.

Key words: MIMO; correlation; coupling; antenna placement.

1. INTRODUCTION

In rich multipath environments, node mobility limits the quality of attainable channel state information (CSI) due to wavelength-scale fast fading, leading to effectively lower channel capacities [2–4]. Analytical results for block fading i.i.d. Gaussian multiple-input multiple-output (MIMO) channels with block length T indicate a severe drop in capacity as T becomes small and that having more than T antennas does not increase capacity [5]. More recent work extends previous results by modeling the MIMO channel with separable transmit/receive correlation. For this case, capacity always increases with additional transmit antennas beyond T, as long as the transmit antennas are correlated. For very rapidly fading channels (T=1) the analysis indicates that antennas should be placed as close together as possible for maximum capacity [1].

One problem with the modeling strategy in [1] is that antenna coupling is neglected, which becomes very important as the inter-element spacing of antennas vanishes. In this paper, the previous analysis is improved by properly accounting for the actual radiated power of the transmit array and not simply constraining the sum of squared antenna currents. This new modeling strategy indicates whether capacity growth results from increased radiated power or from the actual channel. The fundamental observation is that transmit correlation increases capacity through simple beamforming techniques, and that true capacity gain only comes from increased *channel* correlation, not *antenna* correlation whose gain is offset by increased antenna coupling. With these considerations, optimal antenna placement is found to be close to that of conventional phased arrays (0.3 to 0.6 wavelengths).

The remainder of the paper is organized as follows: Section 2 presents the new block fading MIMO channel model. Section 3 introduces the concept of radiated power derived from electromagnetic considerations. Section 4 analyzes capacity increase with correlation in terms of beamforming mechanisms and reveals new conditions for capacity growth. Section 5 discusses optimal antenna placement for rapidly fading channels. Section 6 concludes the paper.

2. CHANNEL MODEL

As in [1, 5], we adopt the block-fading modeling framework

$$\mathbf{X} = \sqrt{(\rho/P)}\mathbf{S}\mathbf{H} + \mathbf{W}, \tag{1}$$

where $\mathbf{S}$ is the $T\times M$ matrix of complex baseband transmit signals, $\mathbf{H}$ is a single realization of the $M\times N$ channel transfer matrix, $\mathbf{X}$ is the $T\times N$ matrix of receive samples, T is the block length, M and N are the number of transmit and receive antennas, and ρ is the average signal to noise ratio (SNR). The new term P represents the average power generated per unit time by the signal matrix $\mathbf{S}$, thus allowing the radiated power to be properly scaled. The $T\times N$ matrix $\mathbf{W}$ of noise samples consists of i.i.d. elements $W_{ij} \sim \mathcal{CN}(0,1)$, with $\mathcal{CN}(\mu,\sigma^2)$ denoting the univariate complex Gaussian distribution with mean μ and variance σ^2.

Proc. 'EuCAP 2006', Nice, France
6–10 November 2006 (ESA SP-626, October 2006)

The channel $\mathbf{H}$ is assumed to be constant over blocks of length T, with elements given by the Kronecker model, or

$$\mathbf{H} = \mathbf{R}_T^{1/2} \mathbf{H}_w \mathbf{R}_R^{1/2}, \tag{2}$$

where $\mathbf{R}_T = (1/N)\mathrm{E}\left\{\mathbf{H}\mathbf{H}^H\right\}$ and $\mathbf{R}_R = (1/M)\mathrm{E}\left\{\mathbf{H}^H\mathbf{H}\right\}$ are the transmit and receive covariance matrices, and $H_{w,ij} \sim \mathcal{CN}(0,1)$. Covariance matrices are generated in this work with a directional channel model, where the probability density function (pdf) of departures or arrivals at angle ϕ in the azimuthal plane is $p(\phi)$. For a uniform linear array (ULA) of Hertzian dipoles, the covariance matrix (for either transmit or receive) has elements

$$R_{ik} = \int_0^{2\pi} d\phi \, p(\phi) \exp[j2\pi(i-k)\Delta x \cos\phi], \tag{3}$$

where Δx is the inter-element spacing in wavelengths.

To understand the effects of different multipath distributions, three forms of $p(\phi)$ at transmit are considered:

1 For full angular spread $p(\phi) = 1/(2\pi)$, and the covariance elements become $R_{T,ik} = J_0[2\pi\Delta x(i-k)]$, where $J_0(\cdot)$ is the zeroth order Bessel function.

2 For a set of L discrete paths with powers β_ℓ and arrival/departure angles ϕ_ℓ, we have

$$R_{T,ik} = \sum_{\ell=1}^{L} \beta_\ell \exp[j2\pi\Delta x(i-k)\cos\phi_\ell]. \tag{4}$$

3 For a single von Mises cluster [6],

$$R_{T,ik} = I_0\left(\sqrt{\kappa^2 - y^2 + j2\pi\kappa y\cos\overline{\phi}}\right)/I_0(\kappa), \tag{5}$$

where $y = 2\pi(i-k)\Delta x$, $\overline{\phi}$ is the mean cluster departure angle, and $\kappa \in [0,\infty)$ controls the cluster width.

3. RADIATED POWER

In MIMO analyses, the transmit signal is typically constrained to have unit average power for each antenna and symbol time [1, 5], or

$$P = P_{\mathrm{tr}} = (1/T)\mathrm{E}\mathrm{Tr}\left\{\mathbf{S}\mathbf{S}^H\right\} = M, \tag{6}$$

where $\mathrm{E}\{\cdot\}$, $\mathrm{Tr}\{\cdot\}$, and $\{\cdot\}^H$ represent expectation, trace, and conjugate transpose respectively. In a realistic system, this is equivalent to constraining the sum of the squared currents on the antenna elements, which for uncoupled antennas also constrains the radiated power. When the antenna elements are electromagnetically coupled, the power radiated during the ith symbol time becomes [7]

$$P_i = \mathbf{s}_i \mathbf{A} \mathbf{s}_i^H, \tag{7}$$

where $\mathbf{A}$ is an $M \times M$ coupling matrix, and $\mathbf{s}_i$ is the ith row of $\mathbf{S}$. The average radiated power per unit time is therefore expressed as

$$P = P_{\mathrm{rad}} = (1/T)\mathrm{E}\mathrm{Tr}\left\{\mathbf{S}\mathbf{A}\mathbf{S}^H\right\}. \tag{8}$$

To simplify the analysis, we assume a ULA of Hertzian dipoles, oriented perpendicular to the azimuthal plane, giving $A_{ij} = J_0[2\pi\Delta x(i-j)]$. Although the assumption of Hertzian dipoles appears to limit the generality of the results, we have also applied precisely the same analysis to more realistic half-wave dipoles analyzed with detailed finite-difference time-domain (FDTD) simulations, and these results will appear in a future article. Since the conclusions are basically identical for Hertzian and half-wave dipoles, the simple assumption does not appear to severely limit the present analysis.

In the development that follows, we assume that the signaling strategy $\mathbf{S}$ is chosen by letting $P = P_{\mathrm{tr}} = M$ as in (6) and then scaling $\mathbf{S}$ so that the radiated power computed in (8) achieves the desired value. This method is suboptimal, since the optimal solution would find $\mathbf{S}$ by directly constraining the radiated power [8]. However, the suboptimal scheme is convenient for this present analysis since it reveals the source of the gains in [1] and whether such gains are realistic.

4. BEAMFORMING AND CAPACITY GROWTH

Understanding the behavior of capacity for correlated block-fading channels is facilitated by an eigenbeamforming interpretation. Substituting (2) into (1) and taking the eigenvalue decomposition (EVD) of the covariance matrices ($\mathbf{R}_P = \boldsymbol{\xi}_P \boldsymbol{\Lambda}_P \boldsymbol{\xi}_P^H$) yields

$$\mathbf{X} = \sqrt{\frac{\rho}{P}}\mathbf{S}\mathbf{R}_T^{1/2}\mathbf{H}_w\mathbf{R}_R^{1/2} + \mathbf{W}, \qquad \text{or} \tag{9}$$

$$\underbrace{\mathbf{X}\boldsymbol{\xi}_R}_{\mathbf{X}'} = \sqrt{\frac{\rho}{P}}\underbrace{\mathbf{S}\,\boldsymbol{\xi}_T}_{\mathbf{S}'}\boldsymbol{\Lambda}_T^{1/2}\underbrace{\boldsymbol{\xi}_T^H\mathbf{H}_w\boldsymbol{\xi}_R}_{\mathbf{H}_w'}\boldsymbol{\Lambda}_R^{1/2}\underbrace{\boldsymbol{\xi}_R^H\boldsymbol{\xi}_R}_{\mathbf{I}} + \underbrace{\mathbf{W}\boldsymbol{\xi}_R}_{\mathbf{W}'}. \tag{10}$$

The unitary transformations do not change the statistics of the channel and noise nor the capacity [5], resulting in the simplified model

$$\mathbf{X}' = \sqrt{\frac{\rho}{P}}\mathbf{S}'\boldsymbol{\Lambda}_T^{1/2}\mathbf{H}_w\boldsymbol{\Lambda}_R^{1/2} + \mathbf{W}. \tag{11}$$

Note that since $\mathbf{H}_w'$ and $\mathbf{W}'$ have the same statistics as $\mathbf{H}_w$ and $\mathbf{W}$, respectively, the primes have been dropped. The behavior of the channel is depicted graphically in Figure 1.

Equation (11) indicates that correlation ($\boldsymbol{\Lambda}_{\{T,R\}} \neq \mathbf{I}$) allows the transmitter and receiver to form beams that excite the spatial modes of the channel with the highest

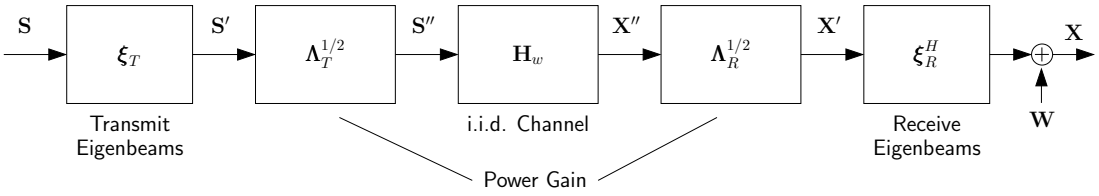

Figure 1. Graphical representation of channels with separable (Kronecker) correlation

gain, referred to commonly as *dominant modes*. From a physical perspective, communicating on the dominant modes corresponds to transmitting and receiving power in directions of high multipath. Adding more antennas allows improved control of the radiation and reception patterns and therefore improved spatial filtering. Thus, the dominant modes of the covariance become stronger as antennas are added, yielding higher beamforming gain and leading to the guaranteed capacity growth in [1].

A logical observation from [1] is that mutual information only depends on the distribution of $\mathbf{S}\mathbf{R}_T\mathbf{S}^H = \mathbf{S}'\mathbf{\Lambda}_T\mathbf{S}'^H$. This fact allowed a scheme to be developed in [1] where mutual information remains constant with added antennas even though the transmit power is reduced. Here we review this analysis and study the impact of including radiated power.

4.1. Effective Power Gain

From the perspective of Fig. 1, for a fixed capacity achieving $\mathbf{S}''$, mutual information only depends on the temporal correlation $\mathbf{S}''\mathbf{S}''^H$ of signals transmitted through the channel. Consider adding ΔM transmit antennas to a system consisting of M antennas ($M \geq T$). Transmit signals can be rearranged so that the first M columns of $\mathbf{S}''$ remain the same, but the additional ΔM columns are zero, meaning no change in the spatio-temporal excitation.

Given a system with M transmit antennas and an abstract quantity $(\cdot)$ (such as $\mathbf{R}_T$, $\mathbf{S}$, etc.), let $\hat{(\cdot)}$ represent the same quantity for $M + \Delta M$ transmit antennas. For Hertzian dipoles, the radiation patterns do not change with additional elements, and the transmit covariance for the $M + \Delta M$ antenna system has the form

$$\hat{\mathbf{R}}_T = \begin{bmatrix} \mathbf{R}_T & \mathbf{Q} \\ \mathbf{Q}^H & \mathbf{R} \end{bmatrix}, \tag{12}$$

with corresponding eigenvalues

$$\hat{\mathbf{\Lambda}}_T = \begin{bmatrix} \hat{\mathbf{\Lambda}}_{T,M} & 0 \\ 0 & \hat{\mathbf{\Lambda}}_{T,\Delta M} \end{bmatrix}, \tag{13}$$

where $\{\cdot\}_M$ and $\{\cdot\}_{\Delta M}$ represent the upper left $M \times M$ and lower right $\Delta M \times \Delta M$ sub-blocks of the matrix, respectively. Mutual information remains constant if the signaling matrix is rearranged as $\hat{\mathbf{S}}'' = [\mathbf{S}''\ \mathbf{0}_{T\times\Delta M}]$, which is equivalent to

$$\hat{\mathbf{S}}' = [\mathbf{S}'\mathbf{\Lambda}_T^{1/2}\hat{\mathbf{\Lambda}}_{T,M}^{-1/2}\ \mathbf{0}_{T\times\Delta M}]. \tag{14}$$

To assess the impact of signal reassignment on the radiated power, we define the effective gain of adding ΔM antennas using the ratio of radiated powers, or

$$G_{\text{eff}} = \frac{\text{ETr}\left\{\mathbf{S}\mathbf{A}\mathbf{S}^H\right\}}{\text{ETr}\left\{\hat{\mathbf{S}}\hat{\mathbf{A}}\hat{\mathbf{S}}^H\right\}}. \tag{15}$$

Thus, if adding the ΔM antennas decreases radiated power, G_{eff} will be greater than unity, indicating capacity growth.

4.1.1. Full Angular Spread

Consider the case of full angular spread with transmit covariance $R_{T,ij} = J_0[2\pi\Delta x(i-j)]$. Since in this circumstance $\mathbf{R}_T = \mathbf{A}$, the radiated power for M antennas is simply $P_{\text{rad}} = (1/T)\text{ETr}\left\{\mathbf{S}'\mathbf{\Lambda}_T\mathbf{S}'^H\right\}$, meaning that beamforming gain is accompanied by a commensurate increase in radiated power, or $G_{\text{eff}} = 1$ indicating no capacity increase. This case highlights one of the key features of systems with mutual coupling: changing the transmit antenna configuration can only enhance beamforming gain if the increase in correlation is not offset by increased coupling.

4.1.2. Single Departure

Next consider the case where propagation to the receiver occurs for only a single departure direction ϕ with $L = 1$ and $\beta_1 = 1$. In this case, a single spatial transmission mode exists given by the eigenvalue and eigenvector pair

$$\lambda = M, \qquad \text{and} \tag{16}$$

$$v_i = 1/\sqrt{M}\exp(j2\pi i\Delta x\cos\phi), \tag{17}$$

respectively. Optimal transmission involves exciting this mode with $\mathbf{S} = \mathbf{s}'\mathbf{v}^H$, where $\mathbf{s}'$ is the vector of time symbols for the current block, producing a radiated power of

$$P_{\text{rad}} = \underbrace{(1/T)\text{E}\left\{\mathbf{s}'^H\mathbf{s}'\right\}}_{=1}\text{Tr}\left\{\mathbf{v}^H\mathbf{A}\mathbf{v}\right\}\lambda^{-1}. \tag{18}$$

Assuming $A_{ij} = J_0[2\pi\Delta x(i-j)]$, we have

$$\text{Tr}\left\{\mathbf{v}^H\mathbf{A}\mathbf{v}\right\} \tag{19}$$
$$= 1 + \frac{1}{M}\sum_{m=1}^{M-1}(M-m)\cos(2\pi m\Delta x\cos\phi)J_0(2\pi m\Delta x).$$

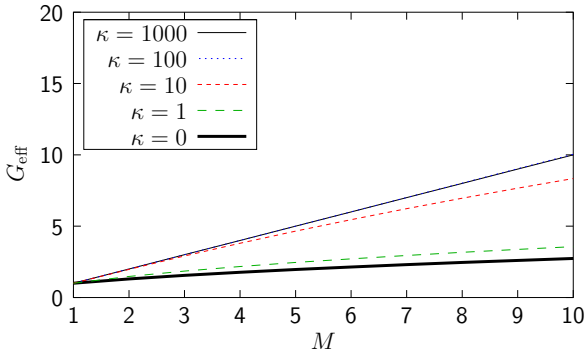

Figure 2. Effective gain versus the number of antenna elements for a single endfire cluster for uncoupled antennas

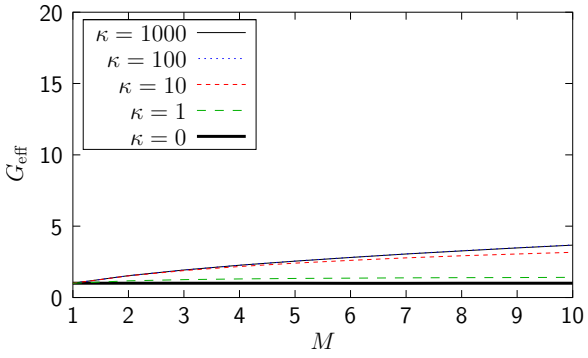

Figure 3. Effective gain versus the number of antenna elements for a single endfire cluster for coupled antennas

By placing antenna elements sufficiently far apart, a gain of M is obtained, which is expected from basic array gain concepts.

4.1.3. von Mises Cluster

Consider the case of a single continuous cluster of departures described by the von Mises distribution with covariance (5). Assuming communication on just the single dominant spatial mode, the effective gain is

$$G_{\text{eff}} = \frac{\mathbf{v}_1^H \mathbf{A} \mathbf{v}_1}{\lambda_1 \hat{\lambda}_1^{-1} \hat{\mathbf{v}}_1^H \hat{\mathbf{A}} \hat{\mathbf{v}}_1}, \tag{20}$$

where λ_1 and $\mathbf{v}_1$ are the principal eigenvalue and corresponding eigenvector of $\mathbf{R}_T$, respectively.

Fig. 2 and 3 plot the effective gain for uncoupled and coupled antennas, respectively, where a single cluster departs in the endfire direction ($\overline{\phi} = 0$), antenna spacing is $\Delta x = 0.5$, and various values of κ are considered. For uncoupled antennas, the capacity growth is inversely proportional to κ, and for $\kappa \to \infty$ effective gain approaches M just as in the case of a single departure. For coupled antennas, the case $\kappa = 0$ (equivalent to full angular spread) has no effective gain. Coupling also inhibits the effective gain for the other values of κ, mainly because the endfire excitation tends to increase radiated power relative to the uncoupled case for $\Delta x = 0.5$. On the other hand, for broadside excitation (not plotted), the coupling actually enhances the effective gain for $\Delta x = 0.5$.

5. ANTENNA PLACEMENT FOR RAPID FADING

For rapidly fading channels ($T = 1$), the results of [1] indicate that only one spatial mode (or beam) should be used and therefore antenna placement should be chosen to maximize the principal channel eigenvalue. Equation (3) indicates that this is accomplished by letting $\Delta x \to 0$ so that $R_{T,ij} \to 1$, producing a single nonzero eigenvalue of M. This concept of placing antennas as close together as possible is troubling from an electromagnetic perspective, since for $\Delta x = 0$ the antennas should function as a single element.

The apparent contradiction arises because the traditional power constraint (6) is not useful for close spacings, due to coherent addition of the fields [7]. For example, for $\Delta x = 0$, $A_{ij} = 1$, meaning that excitation along the principal eigenvector leads to $P_{\text{rad}} = M$ (which equals the channel eigenvalue). Thus, the gain increase is mirrored by a commensurate increase in radiated power, and no true gain is actually present over the single antenna. The following analysis studies this issue in more detail.

5.1. Effective Gain for $M = 2$

For $M = 2$ the transmit covariance matrix is of the form

$$\mathbf{R}_T = \begin{bmatrix} 1 & \gamma \\ \gamma^* & 1 \end{bmatrix}, \tag{21}$$

with eigenvalues $\lambda_{1,2} = 1 \pm |\gamma|$ and eigenvectors

$$\mathbf{v}_{1,2} = (1/\sqrt{2})[1 \quad \pm \exp(-j\angle\gamma)]^T, \tag{22}$$

where $\{\cdot\}^T$ denotes transpose. We consider the case identical to [1], where for $T = 1$ we use $\mathbf{S} = \mathbf{s}'\mathbf{v}_1^H$. For uncoupled antennas, the gain of two antennas over a single antenna is the eigenvalue $\lambda_1 = 1 + |\gamma|$. In our case, however, the transmit signals must be divided by the square root of the factor

$$\begin{aligned} P_{\text{rad}}/P_{\text{tr}} = (1/M)P_{\text{rad}} &= (1/M)\text{ETr}\left\{\mathbf{S}\mathbf{A}\mathbf{S}^H\right\} \\ &= \underbrace{(1/M)\text{E}\left\{\mathbf{s}'^H\mathbf{s}'\right\}}_{=1} \mathbf{v}_1^H \mathbf{A} \mathbf{v}_1, \end{aligned} \tag{23}$$

leading to $G_{\text{eff}} = \lambda_1/(\mathbf{v}_1^H \mathbf{A} \mathbf{v}_1)$. For Hertzian dipoles

$$G_{\text{eff}} = \frac{1 + |\gamma|}{1 + \cos(\angle\gamma) J_0(2\pi\Delta x)}. \tag{24}$$

Thus, we are left with finding the antenna spacing that maximizes the effective gain.

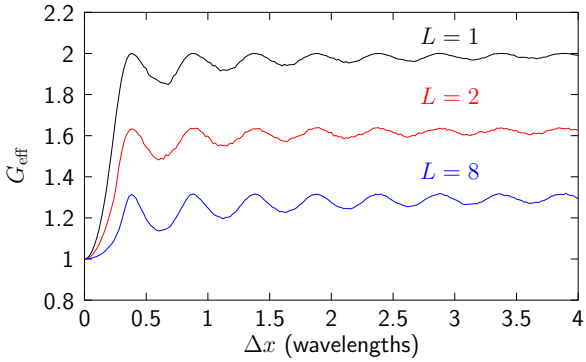

Figure 4. Effective gain for the L-path model from Monte Carlo simulations

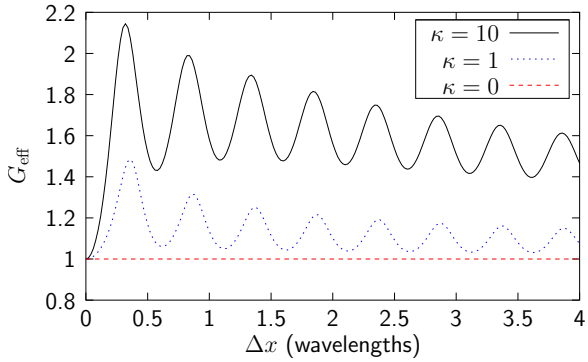

Figure 5. Effective gain as a function of antenna spacing assuming a single departing cluster distributed according to the von Mises distribution for three values of κ with $\overline{\phi} = 0$

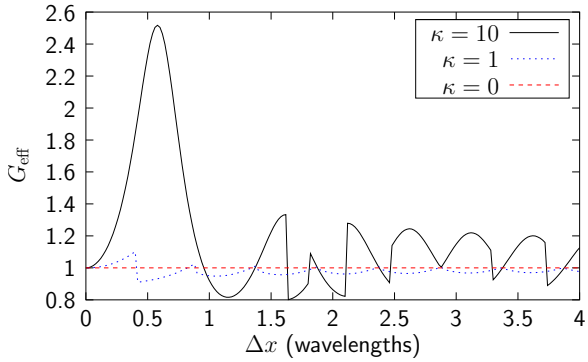

Figure 6. Effective gain as a function of antenna spacing assuming a single departing cluster distributed according to the von Mises distribution for three values of κ with $\overline{\phi} = \pi/2$

5.1.1. Full Angular Spread

The case of full angular spread is trivial, since $\gamma = J_0(2\pi\Delta x)$, and (24) gives $G_{\text{eff}} = 1$, regardless of the antenna spacing. Thus, any increase in correlation due to reduced spacing is exactly offset by an increase in radiated power. To avoid difficulties with element coupling, antenna spacing should be as large as possible.

5.1.2. L-path Model

Next we consider the case of L discrete paths, each having a mean power of $1/L$. The path directions ϕ_ℓ are assumed to be i.i.d. uniform on $[0, 2\pi]$. Fig. 4 plots the mean effective gain computed by averaging G_{eff} over 10^4 channel realizations as a function of spacing. As expected, the effective gain decreases with increasing multipath. Also, antennas should be placed no closer than about 0.4 wavelengths since coupling begins to counteract the benefits of correlation leading to a reduction in G_{eff}.

5.1.3. Von Mises Cluster

Consider a single departing cluster described with a von Mises angular distribution, where $\overline{\phi}$ and κ are fixed. For a specific array orientation, γ is computed from (5) with $y = -2\pi\Delta x$. Fig. 5 and 6 plot G_{eff} versus Δx for three values of κ for endfire ($\overline{\phi} = 0$) and broadside ($\overline{\phi} = \pi/2$) mean departure angle, respectively.

The results reveal that increased multipath causes a gain reduction. However, in contrast to the results observed for the discrete path model, very large spacings are now less desirable. This behavior likely stems from the fixed mean departure angle, as the effective gain averaged over a uniformly distributed sequence of mean departure angles looks similar to the curves for the discrete path model. The key observation from this result is that if array orientation relative to the multipath can be controlled, close spacings may be advantageous. When the arrival angles are more random, very wide spacings appear to be nearly as optimal as narrow spacings.

For a realistic cluster size of 14° ($\kappa = 10$), the optimal spacing for endfire and broadside departures is approximately 0.3 and 0.6 wavelengths, respectively. The optimality of these spacings can be understood by phasing the two antennas such that the main beam is steered in direction $\overline{\phi}$, or $\mathbf{v}^H = (1/\sqrt{2})[1 \ \exp(j2\pi\Delta x \cos\overline{\phi})]$. The resulting radiation pattern of the array is

$$P(\phi) = \cos^2[\pi\Delta x(\cos\phi - \cos\overline{\phi})]. \qquad (25)$$

and is depicted in Fig. 7 and 8 for endfire and broadside excitations, respectively. At spacings of 0.3 and 0.6 wavelengths the radiation pattern has a single main lobe (with virtually no side lobes) in the endfire and broadside directions, respectively. For very wide spacings, the radiation patterns consist of grating lobes, which are undesirable since they emit power away from the main cluster. On the other hand, the radiation patterns for very narrow spacings are nearly uniform, also reducing the spatial selectivity.

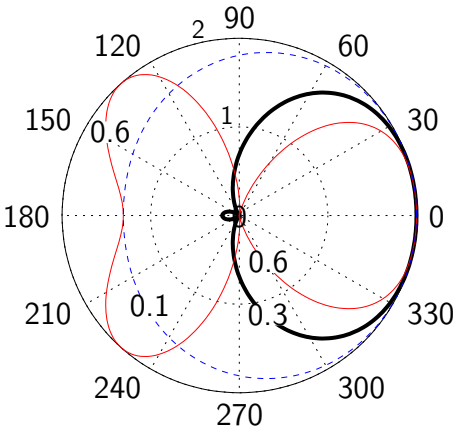

Figure 7. Radiation patterns for endfire excitation ($\overline{\phi} = 0$) on a 2-element array for antenna spacings $\Delta x = \{0.1, 0.3, 0.6\}$ (wavelengths)

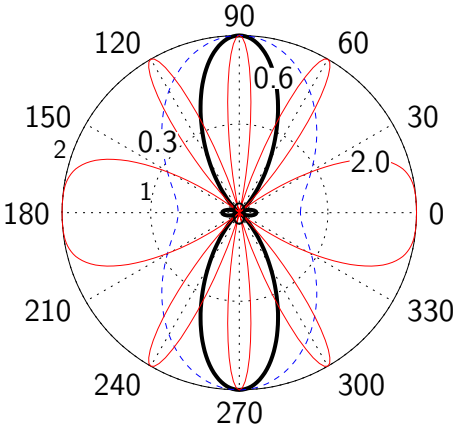

Figure 8. Radiation patterns for broadside excitation ($\overline{\phi} = \pi/2$) on a 2-element array for antenna spacings $\Delta x = \{0.3, 0.6, 2.0\}$ (wavelengths)

5.1.4. von Mises Cluster with Input Power Constraint

One of the strange aspects of the effective gain curves for broadside excitation in Fig. 6 is the presence of discontinuities. These artifacts appear as γ (which is purely real for $\overline{\phi} = \pi/2$) changes sign abruptly as the spacing increases, meaning that signaling changes between even and odd-mode array excitation. This observation highlights the suboptimality of communicating on the principal eigenvector of $\mathbf{R}_T$ and ignoring the effect of antenna coupling in signal construction.

To explore the idea of optimal signaling with covariance information, consider only constraining the signal matrix $\mathbf{S}$ such that $P = P_{\text{rad}} = M$. This constraint can be transformed into the traditional power constraint by making the substitution $\mathbf{S} = \mathbf{S}'\mathbf{A}^{-1/2}$, and the relationship for the channel becomes

$$\mathbf{X} = \sqrt{\frac{\rho}{M}}\mathbf{S}' \underbrace{\mathbf{A}^{-1/2}\mathbf{R}_T^{1/2}}_{\mathbf{R}_T'^{1/2}} \mathbf{H}_w \mathbf{R}_R^{1/2} + \mathbf{W}, \tag{26}$$

thus creating the effective transmit covariance

$$\mathbf{R}_T' = \mathbf{A}^{-1/2}\mathbf{R}_T\mathbf{A}^{-(1/2)H}, \tag{27}$$

which includes both the effects of antenna correlation and coupling. For $T = 1$, the optimal strategy now directs power along the principal eigenvector of $\mathbf{R}_T'$ rather than $\mathbf{R}_T$.

As $\Delta x \to 0$, this strategy is problematic, since the supergain effect becomes significant [8]. To avoid the appearance of impractical supergain solutions, we assume a modified coupling matrix of the form [9]

$$\mathbf{A} = \eta\mathbf{A}_0 + (1-\eta)\mathbf{I}, \;\; \mathbf{R}_T = \eta\mathbf{R}_{T0} \tag{28}$$

where $\mathbf{A}_0$ and $\mathbf{R}_{T0}$ are the radiation-only coupling and covariance matrices defined previously, and η is the antenna radiation efficiency. The first and second terms of $\mathbf{A}$ represent radiation and ohmic loss, respectively. The ohmic loss regularizes the inverse of $\mathbf{A}$, which corresponds to removal of supergain solutions. Since $\mathbf{A}$ now contains loss, the formulation actually constrains the system *input power*.

Assuming $M = 2$, closed-form solutions for G_{eff} with the input power constraint are possible. $\mathbf{A}$ is of the form

$$\mathbf{A} = \begin{bmatrix} 1 & a \\ a^* & 1 \end{bmatrix}, \tag{29}$$

with eigenvalues $\lambda_{1,2} = 1 \pm |a|$ and eigenvectors $\mathbf{v}_{1,2} = (1/\sqrt{2})[1 \pm e^{-j\angle a}]^T$. Thus, having the EVD of $\mathbf{A}$ allows (27) to be computed as

$$\mathbf{R}_T' = \eta \begin{bmatrix} c_1 & c_2 \\ c_2^* & c_1 \end{bmatrix}, \tag{30}$$

with

$$c_1 = b_1^2 + |b_2|^2 + 2\text{Re}\{\gamma b_1 b_2^*\}, \tag{31}$$

$$c_2 = 2b_1 b_2 + \gamma b_1^2 + \gamma^* b_2^2, \tag{32}$$

$$b_1 = [(1+|a|)^{-1/2} + (1-|a|)^{-1/2}]/2, \tag{33}$$

$$b_2 = [(1+|a|)^{-1/2} - (1-|a|)^{-1/2}]\exp(j\angle a)/2, \tag{34}$$

where γ is from (21). The eigenvalues of $\mathbf{R}_T'$ are $\eta(c_1 \pm |c_2|)$. Since the gain of a single antenna is just equal to the efficiency η, the effective gain of two antennas over a single antenna is $c_1 + |c_2|$.

Fig. 9 plots the effective gain versus antenna spacing for a single endfire von Mises cluster with $\kappa = 10$ and different antenna efficiencies (η). The effective gain for the traditional power constraint scaled according to radiated power is also plotted for comparison. The result

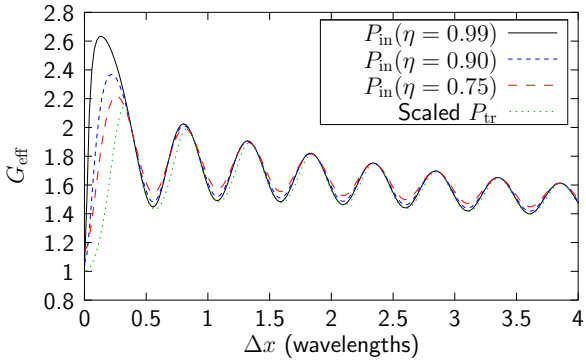

Figure 9. Effective gain for the input-power constraint as a function of antenna spacing assuming a single departing cluster distributed according to the von Mises distribution for $\kappa = 10$ and $\overline{\phi} = 0$

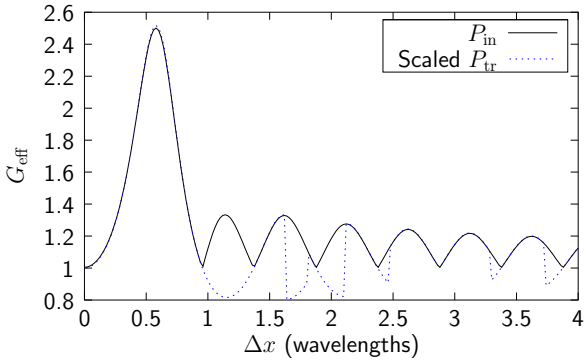

Figure 10. Effective gain for the input-power constraint as a function of antenna spacing assuming a single departing cluster distributed according to the von Mises distribution for $\kappa = 10$ and $\overline{\phi} = \pi/2$

shows that for lower antenna efficiencies the optimal and suboptimal solutions are almost equivalent. As the antenna efficiency increases, however, the optimal spacing approaches zero, indicating the existence of supergain solutions.

Fig. 10 plots a similar result for a single broadside cluster with a fixed efficiency of $\eta = 0.99$. As can be seen, the discontinuities in the effective gain have been removed by the input-power constraint. For narrow spacings, however, the two solutions are nearly identical.

6. CONCLUSION

This paper has explored the effect of applying radiated power considerations to modeling block-fading MIMO channels with Kronecker-type covariance. An analysis of the resulting model indicated that capacity gain results from simple beamforming mechanisms. Also, different conditions were found for capacity growth and optimal antenna placement compared with previous analyses. Gains are only possible when increased correlation is not commensurate with increased coupling. Further, for rapidly fading channels ($T = 1$) radiated power dictates that placing antennas arbitrarily close is equivalent to a single antenna system.

REFERENCES

[1] S. A. Jafar and A. Goldsmith. Multiple-antenna capacity in correlated rayleigh fading with channel covariance information. *IEEE Trans. Wireless Commun.*, 4:990–997, May 2005.

[2] V. Pohl, Phuc Hau Nguyen, V. Jungnickel, and C. von Helmolt. Continuous flat-fading MIMO channels: achievable rate and optimal length of the training and data phases. *IEEE Trans. Wireless Commun.*, 4:1889–1900, July 2005.

[3] A. Goldsmith, S. A. Jafar, N. Jindal, and S. Vishwanath. Capacity limits of MIMO channels. *IEEE Trans. Inf. Theory*, 21:684–702, Jun. 2003.

[4] J. Wallace and M. Jensen. Measurement and characterization of the time variation of indoor and outdoor MIMO channels at 2.4 and 5.2 GHz. In *Proc. 2005 IEEE 62nd Veh. Technol. Conf.*, volume 2, pages 1289–1293, Dallas, TX, Sep. 25-28 2005.

[5] T. L. Marzetta and B. M. Hochwald. Capacity of a mobile multiple-antenna communication link in Rayleigh flat fading. *IEEE Trans. Information Theory*, 45:139–157, Jan. 1999.

[6] A. Abdi, J.A. Barger, and M. Kaveh. A parametric model for the distribution of the angle of arrival and the associated correlation function and power spectrum at the mobile station. *IEEE Trans. Veh. Technol.*, 51:425–434, May 2002.

[7] J. W. Wallace and M. A. Jensen. Mutual coupling in MIMO wireless systems: A rigorous network theory analysis. *IEEE Trans. Wireless Commun.*, 3:1317–1325, Jul. 2004.

[8] M. Morris, M. Jensen, and J. Wallace. Superdirectivity in MIMO systems. *IEEE Trans. Antennas Propag.*, 53:2850–2857, Sep. 2005.

[9] N. W. Bikhazi and M. A. Jensen. The relationship between antenna loss and superdirectivity in MIMO systems. Technical Report https://dspace.byu.edu/handle/1877/66, Brigham Young University, 2005.